DETECTION AND SIZING OF SHORT FATIGUE CRACKS EMANATING FROM RIVET HOLES

O. Kwon[1] and J.C. Kim[1]
[1] Inha University, Inchon, Korea

Abstract: The initiation and growth of short fatigue cracks in a simulated aircraft structure of AA2024-T3 thin plate with a series of rivet holes was detected by acoustic emission (AE) in real-time and the accurate crack sizing was subsequently carried out by using surface acoustic wave (SAW) technique. The locations of short fatigue cracks were determined by AE source location technique. For the precise determination of AE source locations, a region-of-interest (ROI) was set around the rivet holes based on the plastic zone size in plane-stress condition. Since the signal-to-noise ratio (SNR) was very low at this early stage of fatigue damage, the wavelet transform de-noising scheme was employed to enhance the SNR, hence the accuracy of AE source location. In reality, the majority of AE signals detected within the ROI appeared to be noises from various origins. The results showed that the effect of structural geometry and SNR should be closely taken into consideration for the accurate evaluation of fatigue damage in the structure. The SAW technique appeared to be practical for the sizing of fatigue cracks at the range down to a millimetre.

Introduction: Since the fatigue damage usually occurs around the rivet holes in aircraft structures, the detection and sizing of short fatigue cracks emanating from rivet holes is extremely important. In addition, it is well known that the growth behaviour of short cracks is quite different from that of long cracks [1]. Various investigations on the monitoring of crack initiation and growth in aluminium thin plates have been conducted using many different methods. Among them AE has been employed to detect the short cracks in the earlier stage of fatigue damage [2-4], whereas other NDT techniques such as eddy current, magnetic flux leakage, and ultrasonic tests are employed to accurately measure the size of detected cracks. To this end the SAW technique can be an effective one because surface acoustic wave is propagating along the surface with most of its energy being confined within a surface layer [5,6]. When short cracks are present at the root of rivet holes, we may set up an ROI based on the plastic zone size under plane-stress condition. The plastic zone size was estimated by Dugdale strip yield model [7].

Experiments: Specimens were prepared from 1.6mm-thick Alclad2024-T3 plates with the lateral dimensions of 350mm×276mm. Five rivet holes of 3.2mm in diameter were machined at the centre arranged horizontally with 20mm-interval as shown in Fig .1(a). Since fatigue cracks are supposed to be initiated at the right and the left edge of

each hole, each of 10 prospective sites is numbered as shown in Fig. 1(b). The sites were observed by travelling microscope in conjunction with the AE measurement during whole period of fatigue tests. Cyclic load was applied at 5Hz with maximum stress of 110MPa and stress ratio of 0.2.

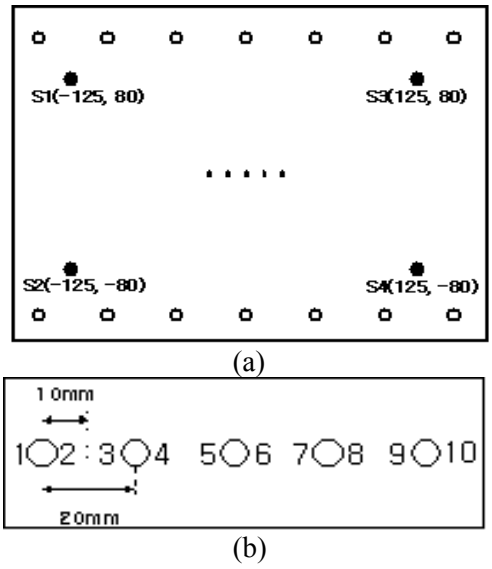

Fig. 1 Geometry of specimens; (a) rivet holes with an array of AE sensors and (b) numbering of prospective crack sites

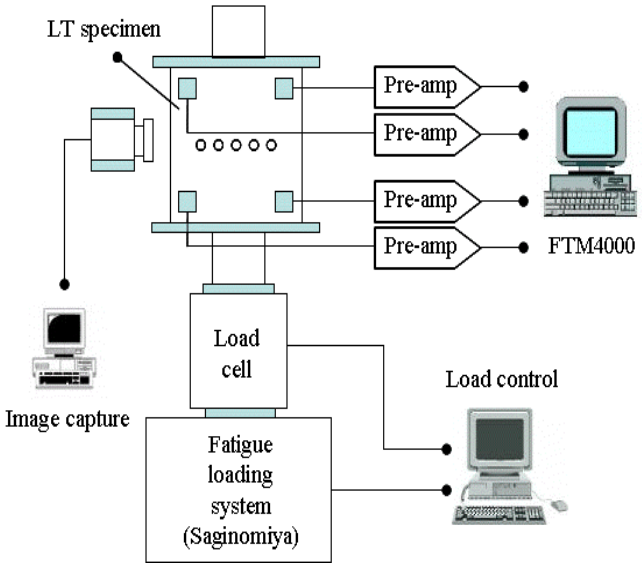

Fig. 2 A schematic diagram of experimental set-up

AE due to fatigue cracks was measured by using a rectangular array of PZT sensors as shown in Fig. 1(a). The sensors have a relatively wide band response between 50kHz and 2MHz. Detected AE signals were amplified 79dB in total and digitised at the sampling frequency of 5MHz to be recorded as digital waveform of 2048 data points. Because the SNR of AE signals at this early stage of fatigue damage was very low, the wavelet transform (WT) was employed to enhance the SNR. WT is a relatively new scheme of frequency-time analysis and was found useful for de-noising of noisy signals such as the signals acquired during fatigue loading [8].

The crack sizing by using the SAW technique was carried out for 4 specimens with fatigue cracks at some rivet holes. An ultrasonic transducer with 10MHz centre frequency was attached to 90º-wedge to generate the surface wave and to receive the reflected signals. The transducer was driven by the pulse generated with a typical pulser-receiver and the received signals were recorded on a digital oscilloscope.

Results and Discussion: The total AE events detected during the fatigue test of 245000 cycles were 5196. Among them about 550 were detected before a crack was observed with the travelling microscope whereas about 4450 were detected after the first crack was discovered. The rest were noises typically found in fatigue tests such as electrical noise, noise due to hydraulic pump, and noise from fixtures connecting specimens and the loading frame. Although the crack growth was more or less continuous showing an exponential type curve with fatigue cycles, AE events occurred intermittently with the initiation and growth of new cracks at different sites to form a stepwise incremental curve of cumulative AE events.

The first crack of 0.47mm was observed at the site 6 at about 193000 cycles. Cracks were subsequently observed at the sites 1 (200100 cycles), 5 (220000 cycles), 9 (223500 cycles), and 10 (224000 cycles). Therefore, the whole period of 245000 cycles was divided into three stages as shown in Fig. 3; (a) before the first crack was observed (0~193000 cycles), (b) from the fist crack observed till the last crack initiated (193000 ~224000 cycles), and (c) after the last crack observed (224000~245000 cycles). The fatigue test was terminated at 245000 cycles when the crack 6 propagated toward the site 7 to connect two adjacent holes. At the site 7 no crack was observed until the abrupt

connection by the approaching crack 6. For each stage, the incremental crack growth and cumulative AE events at individual site were calculated from the result of AE source location.

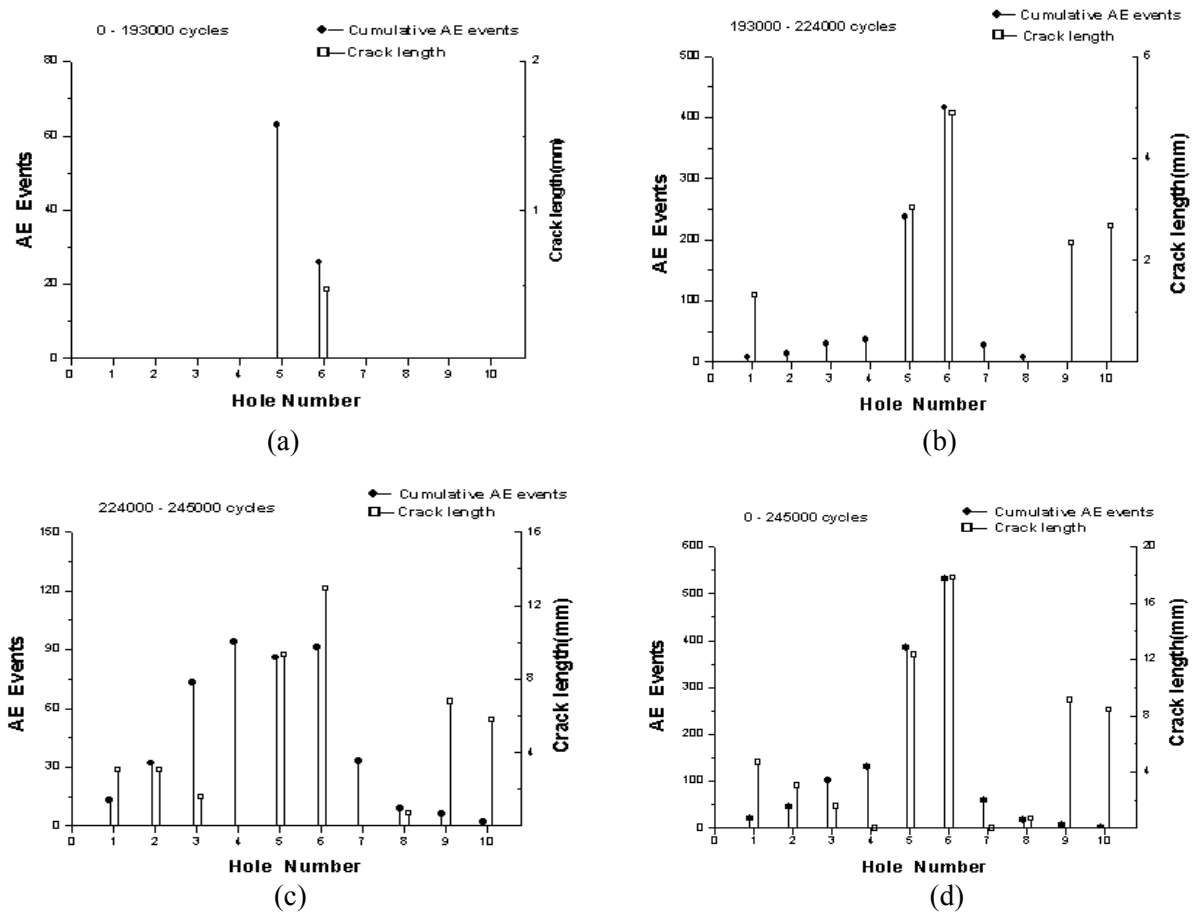

Fig. 3 The incremental crack growth and cumulative AE events at individual site; (a) during 0~193000 cycles, (b) during 193000 ~224000 cycles, (c) during 224000~245000 cycles, and (d) during the entire fatigue test

In Fig. 3(a) some AE events were detected even though no crack was optically observed. These events can be attributed to the initiation of short fatigue cracks too small to be observed by the microscope. In Fig. 3(b) many AE events were detected at the sites 5 and 6 due to the longer crack length, whereas no AE was detected at the sites 9 and 10 although the cracks 9 and 10 were grown to 2.34mm and 2.66mm, respectively. In Fig. 3(c) fewer AE events were detected than in Fig. 3(b) although cracks propagated much faster at many sites. This is because the load bearing capacity decreased with increasing crack length whereas the stress intensity factor at crack tip was increased [2]. It should also be noted that the rates of crack growth and AE events were not exactly corresponding each other as shown in Fig. 3(d), where the crack growth and AE events in Figs. 3(a), 3(b), and 3(c) were summed up to be made for the entire fatigue test.

The sizing of fatigue cracks was carried out in three steps as follows. First of all, the speed of surface wave was measured and the rivet holes in the machined specimens were sized by using the SAW technique. The speed of surface wave was determined as 3077m/s. Then the rivet holes were inspected for the presence of short cracks in the fatigued specimens. Finally, the length of cracks was precisely measured with the information obtained

from the previous steps.

The schematic path of SAW propagation and those reflected signals from an undamaged rivet hole are shown in Fig. 4. The distance from transducer to the centre of the hole was chosen as 15mm. The path difference between

SAW-1 and SAW-2 is equal to the diameter of the hole. In Fig. 4(b), A is a reflection from the interface between transducer and wedge, B is from the interface between wedge and specimen, and C is a reflection from the hole. By expanding the part C with the zooming functions in oscilloscope, Figs. 4(c) and 4(d) show the details of the arrival of reflections. The arrival time difference between SAW-1 and SAW-2 was 1.09 μs, which is equivalent to 3.35mm with the speed of SAW at 3077m/s. The arrival of reflected SAW's in this case were used as the reference for the further evaluation of cracks around the holes in fatigued specimens.

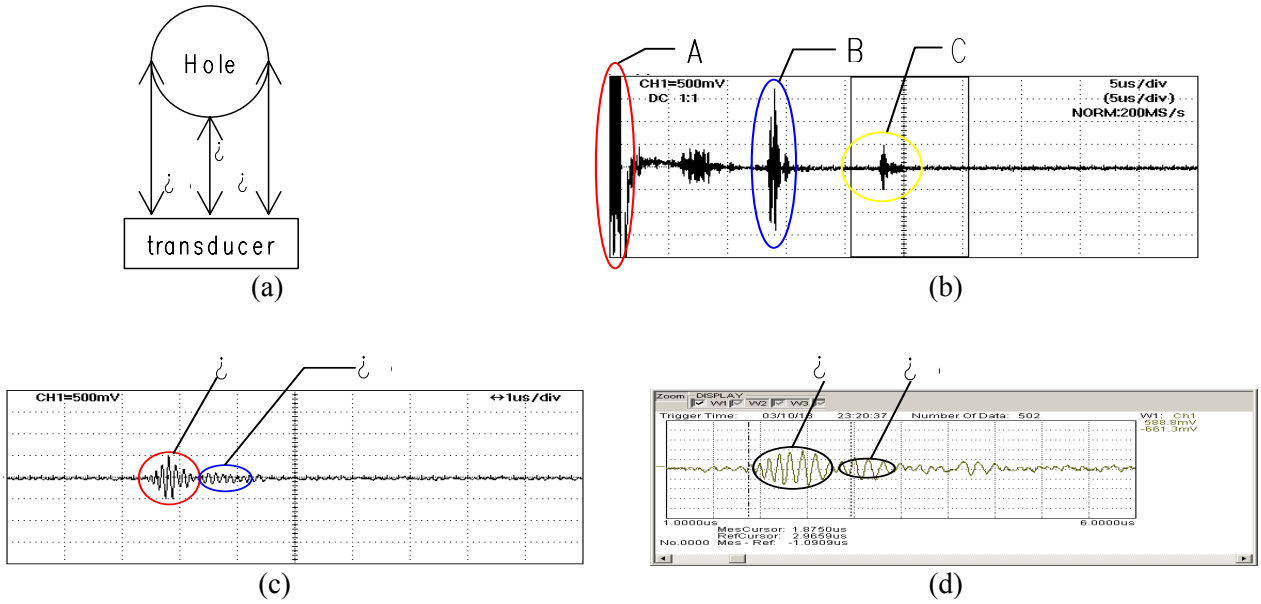

Fig. 4 A result of hole sizing: (a) the schematic of different paths of reflected SAW's, (b) reflected SAW signals recorded at oscilloscope, (c) a zoomed detail of the part C, and (d) a further zoomed detail of part C.

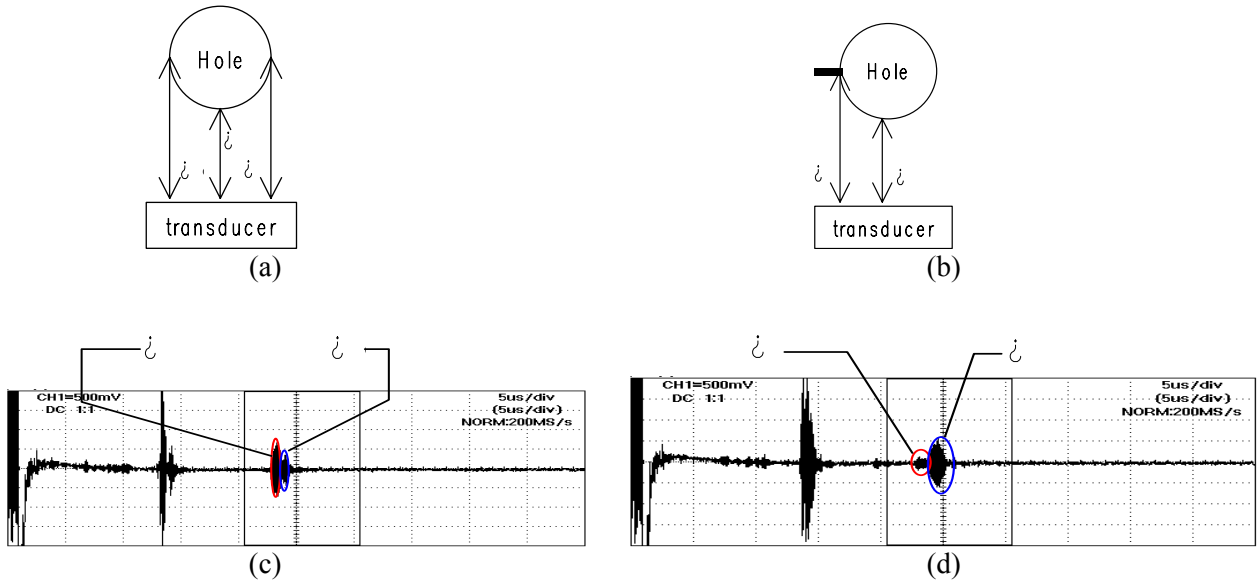

Fig. 5 A result of crack detection: (a) the schematic path and (c) the signals of reflected SAW's with no crack, and (b) the schematic path and (c) the signals of reflected SAW's with a crack.

Fig. 5 shows the test results of SAW inspection for crack detection around the holes. Figs. 5(a) and 5(b) are schematics of the path of SAW propagation around the holes with no crack and with a crack, respectively. Figs. 5(c) and 5(d) are reflected SAW signals from the path in Figs. 5(a) and 5(b), respectively. By comparing with the data in

Fig. 4, the arrival time of both SAW-1 and SAW-2 in Figs. 5(c) and 5(d) are basically the same as those in Fig. 5. The relative amplitudes between SAW-1 and SAW-2 are, however, quite different in Fig. 5(c) and Fig. 5(d). The increased amplitude of SAW-2 in Fig. 5(d) in fact implies the presence of fatigue crack around the hole [9].

The actual sizing of fatigue cracks were conducted on four specimens with various length of fatigue cracks around the holes. Fig 6 shows schematics of the path of SAW propagation around the holes with a crack. SAW-2 could be reflected from the edge of the hole whereas SAW-3 could be reflected from the crack tip as shown in Fig. 6(a). On the other hand, SAW-2' could be a reflection from the crack tip as shown in Fig. 6(b) so that the path difference between SAW-2 and SAW-2' is equal to the crack length. In addition, SAW-2" could be a reflection from the crack tip propagated back to the edge of hole and then detected. The path difference between SAW-2 and SAW-2" is then equal to twice the crack length. Similar schematics are also given in Fig. 6(c).

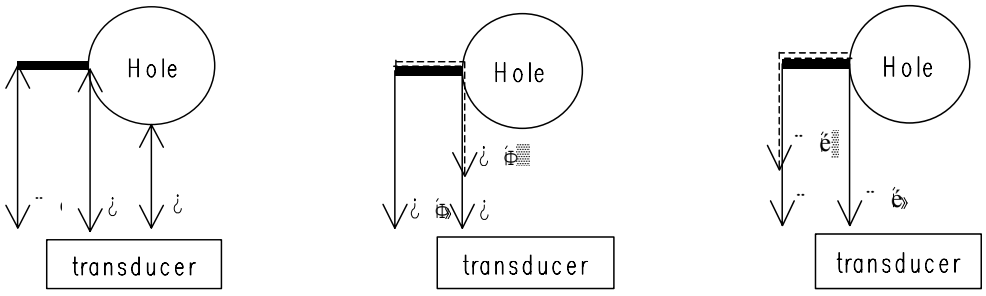

(a) (b) (c)

Fig. 6 Schematics of the path of reflected SAW's: (a) three different paths of plausible reflections of SAW's, (b) various paths of SAW-2, and (c) various paths of SAW-3.

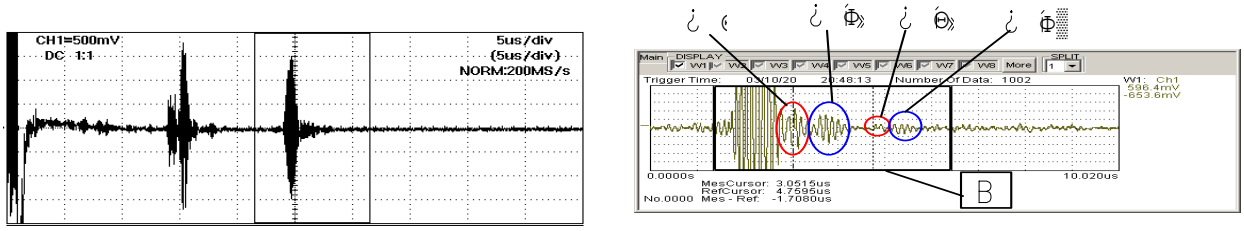

(a) (b)

Fig. 7 A result of crack sizing: (a) a detected signal of reflected SAW's and (b) a zoomed detail of part A.

SAW-1 in Fig. 9 is a reflection from the closest edge of hole toward transducer whereas SAW-2 is a reflection from the crack. The fact that SAW-2 has much higher energy that SAW-1 implies the presence of cracks around the hole. Part A of Fig. 7(a) was expanded to show the details of reflected SAW-2 and SAW-3 as shown in Fig. 7(b). The path difference between SAW-2' and SAW-2" or SAW-3 and SAW-3' is equal to the crack length. From Fig. 7(b) the latter was 1.70 μs, which is equivalent to 5.23mm, whereas the former was 1.59 μs, which is equivalent to 4.98mm. The actual size measured by the microscope was 4.97mm. The bigger error resulted from the crack sizing by SAW-3 was due to the overlap of SAW-2 and SAW-3. On the other hand, SAW-2' and SAW-2" are clearly separated hence resulted in the accurate crack sizing.

In Table 1 the results of crack sizing by SAW technique are summarized with the reference of the measured values by travelling microscope. With the 10MHz ultrasonic transducer employed in this study, cracks of 2~5mm in length were sized most accurately. On the other hand, the crack sizing became inaccurate for the cracks shorter than 2mm or longer than 7mm. When the cracks were short, the energy of reflected SAW was very small so that SAW-2 and SAW-3 were not clearly separated. When the cracks were long enough to result in strong reflections, satellite reflections other than SAW-2 and SAW-3 were detected to be the source of confusion and bigger error.

Especially for the cracks shorter than 1mm, the energy of reflected SAW was too small to be differentiated from noises. For the short fatigue cracks, the crack sizing with transducers of centre frequency at 15 MHz or 25 MHz was also tried with no longer improvement.

Table 1 Results of crack sizing by the SAW technique with the reference of the measured values by travelling microscope

Crack No.	SAW (mm)	Microscope (mm)
1	□	0.30
2	□	0.60
3	□	0.62
4	1.47	1.17
5	1.39	1.2
6	1.57	1.21
7	1.22	1.26
8	2.06	2.12
9	2.65	2.48
10	3.57	3.5
11	4.98	4.97
12	5.42	5.11
13	7.46	7.28

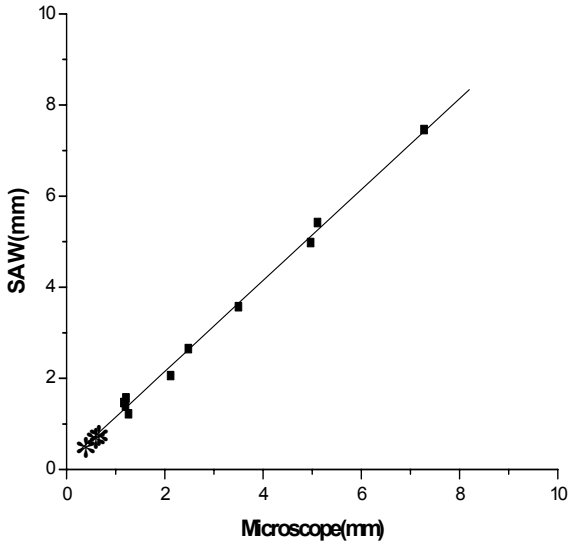

Fig. 8 Comparison of the crack length determined by the SAW technique with the measured values by travelling microscope.

The data shown in Table 1 were plotted in Fig. 8 with the least square fit added. The slope and the intercept at y-axis were 0.9975 and 0.1584, respectively. The crack sizing by the SAW technique resulted in the slightly over-estimation of fatigue cracks [10]. The data points designated as '*' in Fig. 8 denote the crack lengths unable to be sized by the SAW technique.

Conclusions: (1) The rates of crack growth and AE events were not always exactly corresponding each other since AE occurs intermittently with the instantaneous release of stored elastic energy.
(2) The detection of short fatigue cracks around the rivet holes appeared to be practical by comparing the energy of reflected SAW signals with the reference data established for undamaged holes.
(3) The sizing of fatigue cracks in the range of 1~8mm long was possible by using SAW technique with the transducer of centre frequency at 10MHz. The accuracy of sizing was the best for the cracks of 1~8mm in length.
(4) For the cracks shorter than 1mm, the crack sizing appeared to be impossible since the energy of reflected SAW was too small to be differentiated from noises.

References: [1] V. V. Bolotin, *Mechanics of Fatigue*, CRC Press, Boca Raton, Florida (1999), pp. 1-65.
[2] D. M. Granata, P. Kulowitch, W. R. Scott and J. Talia, "Acoustic Emission Waveform Acquisition during Fatigue Crack Growth," *Review of Progress Quantitative NDE*, Vol. 12, 2183-2190 (1993)
[3] K. Ono and J. Y. Wu, "Pattern Recognition Analysis of Acoustic Emission from Fatigue of 2024-T4 Aluminum ," *Progress in Acoustic Emission VIII*, Japanese Soc. NDI, 237-242 (1996)
[4] Z. Shi, J. Jarzynski, S. Bair and L. J. Jacobs, "Study of Acoustic Emission from Incipient Fatigue Failure," *Review of Progress Quantitative NDE*, Vol. 18, 395-401 (1999)
[5] J. Krautkramer and H. Krautkramer, *Ultrasonic Testing of Materials*, Springer-Verlag, Berlin, Germany (1990), pp. 304-307.

[6] Don E. Bray and Don Mcbride, *Nondestructive Testing Techniques*, John Wiley & Sons, Canada (1992), pp. 255-256.
[7] R. W. Hertzberg, *Deformation and Fracture Mechanics of Engineering Materials*, 4th Ed., John Wiley & Sons, New York (1996), pp. 329-330.
[8] K. J. Lee, O. Y. Kwon and Y. C. Joo, "An Improved AE Source Location by Wavelet Transform De-noising Technique", *J. Korean Soc. Nondestructive Testing*, Vol. 20, No. 6, 490-500 (2000)
[9] W. Hassan and W. Veronesi, "Finite element analysis of Rayleigh wave interaction with finite-size, surface - breaking cracks", *Ultrasonics*, Vol. 41, 44-52 (2003)
[10] S. Vanlanduit, P. Guillaume and G. Van Der Linden, "On-line monitoring of fatigue crack using ultrasonic surface waves", *NDT & E International*, Vol. 36, 601-607 (2003)